Analyst

Microfluidic Analysis of Fentanyl-laced Heroin Samples by Surface-enhanced Raman Spectroscopy in a Hydrophobic Medium

Journal:	*Analyst*
Manuscript ID	AN-ART-01-2019-000168.R1
Article Type:	Paper
Date Submitted by the Author:	05-Mar-2019
Complete List of Authors:	Salemmilani, Reza; University of California Santa Barbara, Mechanical Engineering Moskovits, Martin; University of California, Chemistry and Biochemistry 9510 Meinhart, Carl; University of California, Santa Barbara, Department of Mechanical Engineering

SCHOLARONE™
Manuscripts

Microfluidic Analysis of Fentanyl-laced Heroin Samples by Surface-enhanced Raman Spectroscopy in a Hydrophobic Medium

Reza Salemmilani [a], Martin Moskovits [b], Carl D. Meinhart [a,*]

[a] Department of Mechanical Engineering, University of California Santa Barbara, Santa Barbara, California 93106, United States

[b] Department of Chemistry and Biochemistry, University of California Santa Barbara, Santa Barbara, California 93106, United States

* address correspondence to: meinhart@ucsb.edu

Abstract

Opioid overdose deaths resulting from heroin contaminated with the potent opioid agonist fentanyl, are currently a serious public health issue. A rapid and reliable method for identifying fentanyl-laced heroin could lead to reduced opioid overdose. Herein, we describe a strategy for detecting fentanyl at low concentrations in the presence of heroin, based on the significant hydrophobicity of fentanyl compared to heroin hydrochloride, by preferentially extracting trace concentrations of fentanyl using ultrasound-assisted emulsification microextraction using octanol as the extracting phase. Surface-enhanced Raman spectroscopy (SERS), is enabled by exposing the analyte to silver nanoparticle-coated SiO_2 nanoparticles, designed to be stable in mixtures of octanol and ethanol. The sample is then loaded into an SU8/glass microfluidic device that is compatible with non-aqueous solutions. The SERS-active nanoparticles are aggregated by dielectrophoresis using microelectrodes embedded in the microfluidic channels, and the nanoparticle aggregates are interrogated using Raman spectroscopy. Using this method, we were able to reliably detect fentanyl from samples with as low as 1:10,000 (mol mol^{-1}) fentanyl-to-heroin ratio, improving the limits of detection of fentanyl-laced heroin samples by two orders of magnitude over current techniques. The described system could also be useful in chemical detection where rapid and robust preconcentration of trace hydrophobic analytes, and rapid SERS detection in non-aqueous solvents is indicated.

Introduction

Fentanyl is a potent synthetic opioid agonist used medically for acute and chronic management of severe pain and as an adjunct agent for induction and maintenance of general anesthesia. Fentanyl activates opioid receptors in the central nervous system (CNS) and is almost 100 times more potent than morphine [1]. Carfentanil, a fentanyl analogue, is 10,000 times more potent than morphine [2]. This potency is largely due to the very high lipophilicity of fentanyl and its analogues compared to other opioids facilitating their penetration into the CNS [3-5]. Recreational use of fentanyl either in its pure form or more often as fentanyl-laced street heroin and cocaine has greatly increased in the past decade, [6, 7] increasing the incidence of overdose due to the significantly higher potency of fentanyl compared to heroin. From the estimated 72,000 drug overdose deaths in the U.S. in 2017, more than 29,000 were attributed to fentanyl and its analogues up from 10,000 in 2015, making fentanyl the fastest growing overdose causative agent in the current U. S. opioid crisis [6]. Accordingly, rapid, reliable and inexpensive identification of fentanyl-laced heroin would be a valuable tool for reducing accidental opioid overdose deaths resulting from fentanyl and its analogues.

Surface-enhanced Raman spectroscopy (SERS) is a spectroscopic analysis technique shown capable of detecting very low concentrations of analytes [8-13]. Recently, detection of fentanyl in heroin has been reported, where the analyte mixture is exposed to a colloidal SERS substrate [14]. However, when mixtures of analytes are probed using SERS, spectroscopic interference and competition between analytes for adsorption sites on the metallic SERS substrate complicate identification of the substance of interest thereby reducing assay sensitivity. Here we leverage

the difference between the octanol/water partition coefficients of fentanyl and heroin hydrochloride to rapidly and selectively extract fentanyl from fentanyl/heroin mixtures and detect fentanyl, at concentration ratios at least two orders of magnitude lower than what has been previously achieved by SERS [14]. Moreover, our strategy is also applicable to situations where preconcentration of a trace hydrophobic analyte and detection using SERS in a non-aqueous matrix is required.

Extraction and preconcentration of organic molecules from complex aqueous matrices are important sample preparation steps for many analytical chemistry applications. Liquid-liquid extraction (LLE), which is an established technique that often requires large quantities of potentially toxic organic solvents, is oftentimes a lengthy process that may require subsequent evaporation of the extracting organic phase to achieve the desired concentration of the extracted chemical species. Newer techniques such as solid phase microextraction (SPME) [15], and dispersive liquid-liquid microextraction (DLLME) [16] overcome many of the shortcomings of the tradition LLE. More recently, ultrasound-assisted emulsification has been successfully used for microextraction of trace organic molecules from aqueous samples using very low quantities of extracting solvent at significantly improved extraction rates compared to traditional LLE [17-20].

Here, we report a novel technique that enables detection of hydrophobic analytes extracted from aqueous solutions using ultrasound-assisted emulsification microextraction (USAEME) at very low concentrations so as to reliably identify and quantify the analyte by using SERS detection on a microfluidic chip. In our technique, fentanyl is extracted from an aqueous solution containing mixtures of heroin and fentanyl, using octanol as the extracting phase. The octanol containing the extracted fentanyl is then added to an ethanolic colloid of silica nanoparticles decorated with SERS-active silver nanoparticles. The analyte is then loaded into an organic-solvent-compatible

microfluidic chip that uses dielectrophoresis to bring together and immobilize SERS-active nanoparticles. A microscope is subsequently used to probe the nanoparticle trap region and acquire the SERS spectra.

Experimental

Microfluidic Chip Fabrication. Gold electrodes (500 nm-thick) are evaporated by electron beam onto a 500 μm-thick fused silica wafer. Detailed steps for fabricating the electrode substrate were previously reported [8]. Microfluidic inlets and outlets and access ports for the electrode contact pads are etched using 49% hydrofluoric acid (HF) in a 500 μm-thick fused silica backing wafer. The wafer is washed with DI water, dried with nitrogen and cleaned for 10 min in piranha solution (3:1 H_2SO_4:H_2O_2), rinsed with DI H_2O, dried with nitrogen, and immediately submerged in a 2% (v/v) solution of 3-Aminopropyltriethoxysilane (APTES) and 1% (v/v) DI H_2O in ethanol. The pH of the solution is adjusted to ~11 using NH_4OH to catalyze the APTES hydrolysis reaction. The amination reaction is allowed to continue overnight. The wafer is rinsed and sonicated in anhydrous ethanol to remove any physisorbed APTES layer (may appear as a white film) and stored under anhydrous ethanol.

Microfluidic structures are lithographically patterned using SU-8 as the structural material on the electrode substrate. Hard-baking of the SU-8 is avoided to preserve sufficient unreacted epoxide groups on the SU-8 surface for the subsequent amine-epoxide bonding reaction.

The aminated backing wafer is removed from ethanol, dried using N_2, immediately aligned with the SU-8 microchannel substrate, and the two wafers are gently pressed together for a few minutes, resulting in a securely bonded device. The bonded wafers, held together under pressure

using a fixture, are then hard-baked on a hot-plate at 120°C for 30 min. Figure 1 depicts the fabrication steps for the SU-8/glass microfluidic dielectrophoresis chip.

Brass eyelets are epoxied to the inlet and outlet vias to form the fluidic chip-to-world access points. Aluminum wires are soldered to the electrode contact pads to form electrical connections between the chip and the AC signal generator (33220A, Agilent, CA, USA), output of which is amplified using a voltage amplifier (F20A, FLC Electronics, Sweden).

Synthesis of AgNP-coated SiO_2 Nanoparticles. 1.0 ml of 20 nm citrate-capped silver nanoparticles (AgNP) (1.0 mg ml^{-1} biopure, nanoComposix) were washed once and redispersed in MilliQ DI water to reduce the concentration of the citrate buffer in which the AgNPs were initially dispersed. AgNP colloid was then slowly added to 1.5 ml of 400 nm amino-terminated silica nanoparticles at a concentration of 10 mg ml^{-1} (NanoXact, nanoComposix) while sonicating to ensure uniform decoration of the silica nanoparticles with the AgNPs. Sonication was continued for ~ 4 hours followed by centrifugation to remove unbound AgNPs. The AgNP-coated SiO_2 nanoparticles were then washed once with MilliQ H_2O to remove residual citrate and redispersed in ethanol. Figure 2 shows SEM images of the bare aminated SiO_2 nanoparticles (a) and the SiO_2 nanoparticles decorated with AgNPs (b). Figure 2 (c) and (d) show the absorption spectra of the bare SiO_2 nanoparticles and AgNP-coated SiO_2 nanoparticles (in ethanol), respectively.

The SERS substrates, synthesized as described above, are uncapped and, therefore, prone to contamination during synthesis and storage. The AgNP-coated SiO_2 nanoparticles were modified with a solution of 2 mM sodium iodide, immediately before carrying out the chemical detection experiments, forming an iodide monolayer on the silver surfaces, thereby, effectively eliminating

interfering signals arising from adsorbed contaminant molecules. Details of the iodide modification procedure and its utility can be found in a previous publication [8].

Sample Preparation. Chemicals: heroin hydrochloride (Sigma-Aldrich), fentanyl (Sigma-Aldrich), 1-octanol >99.9% purity (Sigma-Aldrich).

Table 1 summarizes the compositions of the samples used for the experiments:

Table 1. Composition of the fentanyl-laced heroin samples.

Sample	Heroin concentration	Fentanyl concentration
(a)	1 mM	100 μM
(b)	1 mM	10 μM
(c)	1 mM	1 μM
(d)	1 mM	100 nM

For the extraction step, 20 μL of octanol is added to 1.0 ml of aqueous solution of the analyte. The sample is vigorously shaken for 30 seconds followed by ultrasonication for 20 min using a benchtop sonicator to emulsify the mixture, significantly speeding up the extraction of the hydrophobic fentanyl into the octanol phase. After extraction, phase-separation is achieved by centrifugation at 4000 rcf for 5 min. The extracted analyte in octanol is then added to the ethanolic AgNP-coated SiO_2 colloid at a ratio of 1:5 (Figure 3a). The AgNP-coated SiO_2 colloid remains stable in a dispersing phase of 1:5 octanol to ethanol.

Raman Spectroscopy. The AgNP-coated SiO_2 colloid/analyte mixture is loaded into the microfluidic chip. Flow is established via vacuum and is adjusted to a low rate of 1 μL min^{-1}. Electrodes are activated at 4.0 MHz and a voltage of 70 V_{pp}. Positive dielectrophoresis (DEP) is

observed as the nanoparticles come together and form so-called "pearl chains" (Figure 3b). The agglomerated SERS-active nanoparticles are then probed using a LabRam Aramis Raman spectrometer (Horiba, Japan) with a 50X objective, exposing the sample to 0.78 mW of 633 nm laser power.

Results and Discussion

Solvent-compatible Microfluidic Chip. We have previously reported using dielectrophoresis for spatial control of SERS-active silver nanoparticles in a PDMS-based microfluidic device [8]. Dielectrophoresis for particle manipulation in microfluidic devices has been extensively studied [21-23]. In brief, particles placed in a non-uniform electric field experience an attractive or repulsive dielectrophoretic force, the direction of which is a function of complex-valued permittivities of the dispersing medium and the particles. The dielectrophoretic force can therefore be utilized, in conjunction with a microfluidic device, to aggregate SERS-active particles, forming hot-spots on-demand [8, 22]. To activate the nanoparticle trap, we apply an AC potential of 70 V_{pp} at 4.0 MHz, causing the nanoparticles to migrate towards the electrode's edges within seconds. This phenomenon is known as positive DEP. Electric fields induced by the nanoparticles attached to the electrodes further enhance the DEP force resulting in the formation of a so called nanoparticle "pearl-chains" (Figure 3b).[24] Applying larger potentials boosts the DEP force in general resulting in reduced trapping time and enhanced performance. However, the applied potential is often limited by complicating factors such as competing electrokinetic effects and water electrolysis.[25] A major advantage of our strategy is that the solvent (octanol/ethanol) does not undergo electrolysis, hence larger potentials (i.e. 70 V_{pp}) can be applied to aggregate

nanoparticles more rapidly (under 10 seconds as seen in Figure 3b). Polydimethylsiloxane (PDMS) is the most common material for fabrication of microfluidic chips using soft-lithography [26-28]. However, PDMS-based microfluidic devices are not compatible with most non-aqueous solvents such as octanol which can cause swelling of the structures and leaching of uncured monomer from PDMS into the organic solvent flow [29]. To avoid this problem, we used SU-8 epoxy resin as the structural material for the microfluidic channels. Amine-epoxide chemistry has been previously used for irreversible chemical bonding of PDMS to SU-8 and sealing microfluidic channels [30, 31]. Here we report, amine-modification of a fused silica substrate using APTES and subsequent irreversible bonding to an SU-8 microfluidic layer to form sealed microfluidic channels. A major advantage of this method is that it is carried out at room temperature, with low applied-pressure bonding, in contrast to glass-to-glass direct wafer bonding which typically requires high temperatures and a high applied pressure. Microfluidic channels formed using this technique showed no evidence of swelling for the duration of the experiments; no chemical contamination from the hard-baked SU-8 was noted; and, no liquid leakage from the channels, air leakage into the channels, or delamination of the SU-8 layer was observed.

AgNP-coated SiO_2 Nanoparticles. Colloids are typically stabilized electrostatically through double-layer interactions, sterically by means of adsorbed polymers or other ligands, or by a combination of both effects [32-34]. Citrate-capped silver nanoparticles are stabilized primarily by electrostatic forces and hence undergo aggregation in many non-aqueous solvents such as octanol. Amine-modified SiO_2 nanoparticles were found to be stable in ethanolic solutions. Very high surface AgNP coverage, while improving the plasmonic properties of the composite nanoparticles, adversely impacted colloidal stability. AgNP coverage of the SiO_2 nanoparticles

was adjusted to render the composite nanoparticles as highly enhancing as possible while preserving their colloidal stability in ethanolic solutions (Figure 2b). The SERS activity of the AgNP-coated SiO_2 nanoparticles are believed to be due to the presence of silver clusters on the surface of the SiO_2 nanoparticles, and, more importantly, to the formation of SERS "hot-spots" pursuant to the aggregation of the nanoparticles by DEP. It was found that addition of octanol to the ethanolic AgNP-coated SiO_2 dispersion at a ratio of 1:5 did not disrupt the stability of the colloid. This is likely due to steric stabilization of the AgNP-coated SiO_2 colloid imparted by aminopropyl chains on the silica surfaces from the APTES condensation reaction during the amination step. Higher octanol concentrations adversely affected stability and were avoided.

Figure 2 depicts the SEM images of the SiO_2 nanoparticles before and after decoration with AgNPs. Surface coverage of the AgNPs on the SiO_2 nanoparticles is relatively uniform owing to sonication during attachment of AgNPs to the aminated SiO_2 nanoparticles. Figure 2(d) shows the absorption spectrum of the AgNP-coated SiO_2 particles. Peak absorbance is observed at ~400 nm which corresponds well to the absorbance spectrum of 20 nm silver nanoparticles [35]. Stability of the AgNP-coated SiO_2 particles in 1:5 octanol to ethanol dispersant is confirmed using dynamic light scattering.

It is worth noting that uncapped/partially capped silver surfaces are very susceptible to contamination. To remove the contaminants that are adsorbed onto the silver surfaces during/after synthesis, the AgNP-coated SiO_2 nanoparticles were modified with I^- immediately prior to use. Iodide modification of silver/gold nanoparticle results in formation of a monolayer of I^- ions on the silver/gold surfaces, effectively displacing from the silver/gold surfaces the adsorbed molecules with potentially interfering Raman spectra, as previously reported by many groups, including ours [8, 36, 37].

Modification of the silver surfaces with I^- did not adversely affect the stability of the nanoparticles. An additional, yet important, advantage of iodide-modification is the appearance of a strong Ag-I vibrational band at ~118 cm^{-1} (Figure S1), the intensity of which correlates well with the degree of aggregation of the SERS-active nanoparticle clusters. We used the intensity of this Ag-I band to normalize the acquired spectra to effectively eliminate the dependence of the intensity of the spectra to the SERS activity of the nanoparticle clusters. Therefore, after normalization, the main parameter influencing the intensity of the signal would be the concentration of the analyte, enabling quantification of the analyte concentration by comparing relevant peak heights.

Solvent Extraction and Raman Spectroscopy. Figure 4 shows the normalized spectra before and after the extraction step with on-chip detection. For the control experiments (before extraction - blue spectra), spectral features assigned to fentanyl (1002 cm^{-1} and 1028 cm^{-1}) are clearly observed down to a 1% fentanyl-to-heroin concentration ratio. At lower fentanyl-to-heroin concentration ratios, spectral features associated with heroin (for example, the band at 624 cm^{-1}) clearly dominate. After extraction, fentanyl bands are clearly seen down to fentanyl-to-heroin concentration ratio of 0.01% while heroin bands are virtually absent.

Figure 5 shows the intensity of 1002 cm^{-1} band (fentanyl) and 624 cm^{-1} band (heroin) for the control samples and the extracted samples. Dashed lines correspond to a signal-to-noise ratio of 3; Bands with intensities below this line are considered unreliable. These results suggest that fentanyl, with an octanol/water partition coefficient of $K_p \sim 717$ is preferentially concentrated in the octanol phase during the extraction process and heroin hydrochloride is depleted from the octanol phase owing to its hydrophilicity (estimated $K_p \sim 0.015$ for its cationic forms) [38, 39].

Figure 5(a) shows that solvent extraction improves the limit-of-detection (LOD) of fentanyl by two orders of magnitude. This improvement in LOD could be due to the increased concentration of fentanyl in the SERS hotspots resulting from the extraction step, and also depletion of high concentration heroin in the sample and hence elimination of the competition between heroin and fentanyl molecules for adsorption sites on the silver surfaces. It is worth noting that for the sample with 10% fentanyl-to-heroin concentration ratio (Figure 4(a)), fentanyl bands are stronger before solvent extraction despite the higher concentration of the analyte in the extracting phase. This suggests that solvent plays an important role in the adsorption process and/or (less likely) the plasmonic properties of the SERS-active silver surfaces. It is important to note that the strategy introduced here can find numerous applications where significant preconcentration of a hydrophobic analyte (e.g. a pesticide) in an aqueous sample (e.g. contaminated groundwater) using solvent extraction is required, and subsequent rapid on-chip chemical analysis by SERS, of the sample in the organic extracting phase is desired.

Conclusion

A novel microfluidic approach is described for the detection of trace hydrophobic analytes in non-aqueous solvents using SERS. Using the approach described, fentanyl at very low concentrations is preferentially extracted from aqueous mixtures of heroin hydrochloride (hydrophilic) and fentanyl (hydrophobic) using octanol as the extracting phase. SERS-active AgNP-coated SiO_2 particles are synthesized, with silver nanoparticle coverage adjusted to maximize enhancement without compromising colloid stability in mixtures of octanol/ethanol. The extracted analyte (fentanyl in octanol) is premixed with the AgNP-coated SiO_2 nanoparticles

and is loaded into an SU-8/glass microfluidic chip that is compatible with organic solvents. Microelectrodes embedded in the microfluidic channels, induce aggregation of the nanoparticles by dielectrophoresis. The trapped AgNP-coated SiO_2 nanoparticles are then probed using a Raman microscope, excited with a 633 nm laser. Extraction of fentanyl from mixtures of fentanyl and heroin improves the LOD of fentanyl by two orders of magnitude, enabling reliable detection of trace amounts of fentanyl in fentanyl-laced heroin samples. The obvious implications of this approach to the reduction of harm from drug overdose are briefly discussed.

Conflict of interest statement

There are no conflicts of interest to declare.

Acknowledgements

The fabrication was undertaken at the UCSB nanofabrication facility, part of the National Science Foundation-funded national nanofabrication infrastructure network. This work was supported in part through grant W911NF-09-0001 from the U.S. Army Research Office at the Edgewood Chemical Biological Center. The content of the information does not necessarily reflect the position or the policy of the Government, and no official endorsement should be inferred.

Supporting Information. Representative, full wavenumber range Raman spectra, normalized by the Ag-I band at ~118 cm^{-1}, before extraction and after extraction.

References

1. J. Suzuki and S. El-Haddad, *Drug Alcohol Depend*, 2017, **171**, 107-116.
2. D. M. Swanson, L. S. Hair, S. R. Strauch Rivers, B. C. Smyth, S. C. Brogan, A. D. Ventoso, S. L. Vaccaro and J. M. Pearson, *J Anal Toxicol*, 2017, **41**, 498-502.
3. NIH, Fentanyl, https://www.drugabuse.gov/publications/drugfacts/fentanyl, (accessed 7/1/2018).
4. R. S. Vardanyan and V. J. Hruby, *Future Med Chem*, 2014, **6**, 385-412.

5. J. Lotsch, C. Walter, M. J. Parnham, B. G. Oertel and G. Geisslinger, *Clin Pharmacokinet*, 2013, **52**, 23-36.
6. NIH, Overdose Death Rates, https://www.drugabuse.gov/related-topics/trends-statistics/overdose-death-rates) accessed 7/1/2018).
7. D. Ciccarone, *Int J Drug Policy*, 2017, **46**, 107-111.
8. R. Salemmilani, B. D. Piorek, R. Y. Mirsafavi, A. W. Fountain, 3rd, M. Moskovits and C. D. Meinhart, *Anal Chem*, 2018, **90**, 7930-7936.
9. C. L. Haynes, A. D. McFarland and R. P. Van Duyne, *Analytical Chemistry*, 2005, **77**, 338a-346a.
10. C. Andreou, M. R. Hoonejani, M. R. Barmi, M. Moskovits and C. D. Meinhart, *ACS Nano*, 2013, **7**, 7157-7164.
11. K. K. Kneipp, Harald; Itzkan, Irving; Dasari, Ramachandra R. , Feld S., Michael, *J. Phys.: Condens. Matter*, **14**, 28.
12. K. L. Wustholz, A. I. Henry, J. M. McMahon, R. G. Freeman, N. Valley, M. E. Piotti, M. J. Natan, G. C. Schatz and R. P. Van Duyne, *J Am Chem Soc*, 2010, **132**, 10903-10910.
13. K. Kneipp, Y. Wang, H. Kneipp, L. T. Perelman, I. Itzkan, R. R. Dasari and M. S. Feld, *Physical Review Letters*, 1997, **78**, 1667-1670.
14. A. Haddad, M. A. Comanescu, O. Green, T. A. Kubic and J. R. Lombardi, *Anal Chem*, 2018, **90**, 12678-12685.
15. C. L. Arthur and J. Pawliszyn, *Analytical Chemistry*, 1990, **62**, 2145-2148.
16. M. Rezaee, Y. Assadi, M. R. M. Hosseinia, E. Aghaee, F. Ahmadi and S. Berijani, *Journal of Chromatography A*, 2006, **1116**, 1-9.
17. J. Regueiro, M. Llompart, C. Garcia-Jares, J. C. Garcia-Monteagudo and R. Cela, *J Chromatogr A*, 2008, **1190**, 27-38.
18. J. F. Wu, B. R. Xiang and J. Xia, *Microchim Acta*, 2009, **166**, 157-162.
19. A. R. Fontana, S. H. Patil, K. Banerjee and J. C. Altamirano, *J Agric Food Chem*, 2010, **58**, 4576-4581.
20. M. Vila, J. P. Lamas, C. Garcia-Jares, T. Dagnac and M. Llompart, *Microchemical Journal*, 2016, **124**, 530-539.
21. B. Cetin and D. Li, *Electrophoresis*, 2011, **32**, 2410-2427.
22. S. Cherukulappurath, S. H. Lee, A. Campos, C. L. Haynes and S.-H. Oh, *Chemistry of Materials*, 2014, **26**, 2445-2452.
23. M. Alshareef, N. Metrakos, E. Juarez Perez, F. Azer, F. Yang, X. Yang and G. Wang, *Biomicrofluidics*, 2013, **7**, 11803.
24. K. D. Hermanson, S. O. Lumsdon, J. P. Williams, E. W. Kaler and O. D. Velev, *Science*, 2001, **294**, 1082-1086.
25. A. Ramos, H. Morgan, N. G. Green and A. Castellanos, *Journal of Physics D: Applied Physics*, 1998, **31**, 2338-2353.
26. J. C. McDonald, D. C. Duffy, J. R. Anderson, D. T. Chiu, H. Wu, O. J. Schueller and G. M. Whitesides, *Electrophoresis*, 2000, **21**, 27-40.
27. G. M. Whitesides, E. Ostuni, S. Takayama, X. Jiang and D. E. Ingber, *Annu Rev Biomed Eng*, 2001, **3**, 335-373.
28. A. Khademhosseini, K. Y. Suh, S. Jon, G. Eng, J. Yeh, G. J. Chen and R. Langer, *Anal Chem*, 2004, **76**, 3675-3681.
29. J. N. Lee, C. Park and G. M. Whitesides, *Anal Chem*, 2003, **75**, 6544-6554.
30. Z. Y. Zhang, P. Zhao, G. Z. Xiao, B. R. Watts and C. Q. Xu, *Biomicrofluidics*, 2011, **5**.
31. Y. Ren, S.-H. Huang, S. Mosser, M. Heuschkel, A. Bertsch, P. Fraering, J.-J. Chen and P. Renaud, *Micromachines*, 2015, **6**, 1923-1934.

32. D. H. Napper, *Journal of Colloid and Interface Science*, 1977, **58**, 390-407.
33. T. R. Sato, R.; , *Surfactant Science Series*, 1980, **9**.
34. J. W. Park and J. S. Shumaker-Parry, *J Am Chem Soc*, 2014, **136**, 1907-1921.
35. S. Agnihotri, S. Mukherji and S. Mukherji, *RSC Adv.*, 2014, **4**, 3974-3983.
36. M. Y. Chan, W. Leng and P. J. Vikesland, *Chemphyschem*, 2018, **19**, 24-28.
37. L. J. Xu, C. Zong, X. S. Zheng, P. Hu, J. M. Feng and B. Ren, *Anal Chem*, 2014, **86**, 2238-2245.
38. R. Gulaboski, M. N. Cordeiro, N. Milhazes, J. Garrido, F. Borges, M. Jorge, C. M. Pereira, I. Bogeski, A. H. Morales, B. Naumoski and A. F. Silva, *Anal Biochem*, 2007, **361**, 236-243.
39. S. D. Roy and G. L. Flynn, *Pharm Res*, 1988, **5**, 580-586.

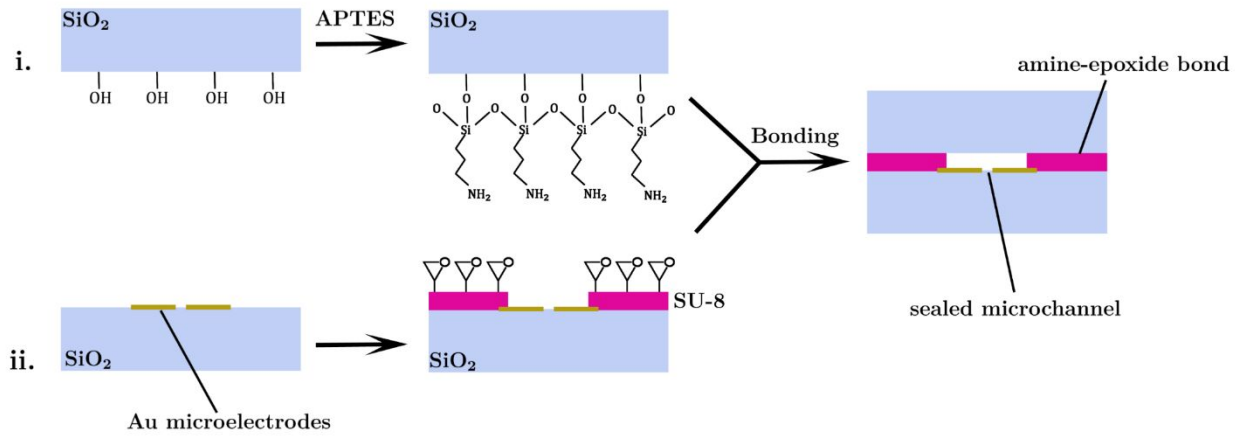

Figure 1. Schematic detailing the fabrication steps of the SU-8/glass microfluidic dielectrophoresis device. The clean (hydroxylated) fused silica backing wafer (i) with etched vias for fluidic inlets and outlets, is aminated using APTES. The SU-8 microchannel features are lithographically patterned on the fused silica electrode substrate (ii) on which the electrode features have been previously fabricated. The two wafers are aligned, brought into contact, and placed on a hot plate at 120 ℃ under applied pressure (15 psi). The reaction between surface epoxide groups on the SU-8 layer and amino groups from the aminopropyl chains create a strong bond that seals the microfluidic channels.

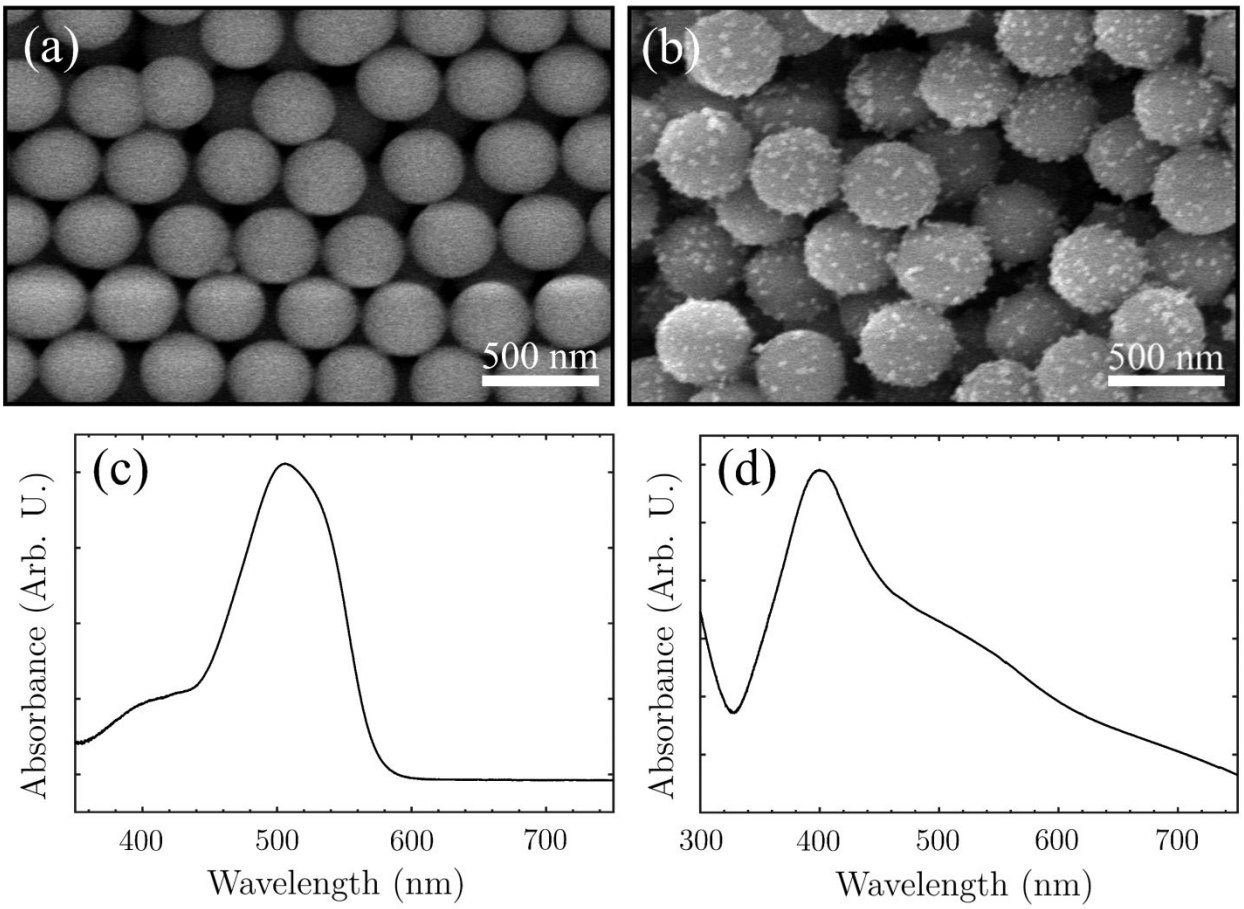

Figure 2. SEM images of 400 nm aminated SiO_2 nanoparticles before (a) and after (b) decoration with 20 nm AgNPs. Surface coverage fraction is adjusted such that the composite nanoparticles are still SERS-active, while retaining stability in ethanol/octanol mixtures. Subplots (c) and (d) depict absorbance of the SiO_2 nanoparticles (in ethanol) before and after decoration with AgNPs, respectively. Absorbance characteristics of the AgNP-coated SiO_2 nanoparticles are dominated by the AgNPs (peak absorbance ~ 400 nm).

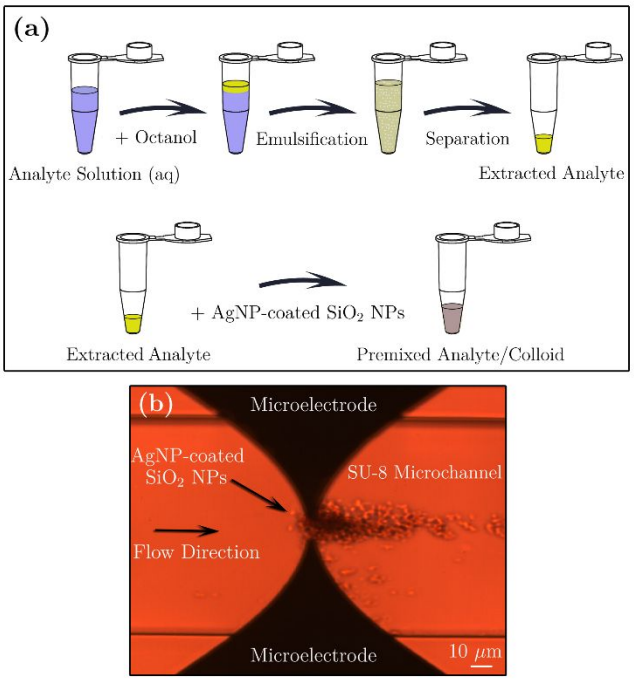

Figure 3. (a): Sample preparation steps: octanol is added to aqueous solution of fentanyl-laced heroin, sample is emulsified by ultrasonication for the extraction of fentanyl from the solution, phase separation is achieved by centrifugation, and the extracted fentanyl (in octanol) is premixed with the AgNP-coated 400 nm SiO_2 nanoparticles that are dispersed in ethanol. (b): The analyte is loaded into the microfluidic device and the nanoparticles are captured by applying an electric potential to the gold microelectrodes. Microelectrodes are embedded within an SU-8/glass microchannel that is compatible with organic solvents. The Trap is probed using a Raman microscope and spectra are acquired (Figure 4).

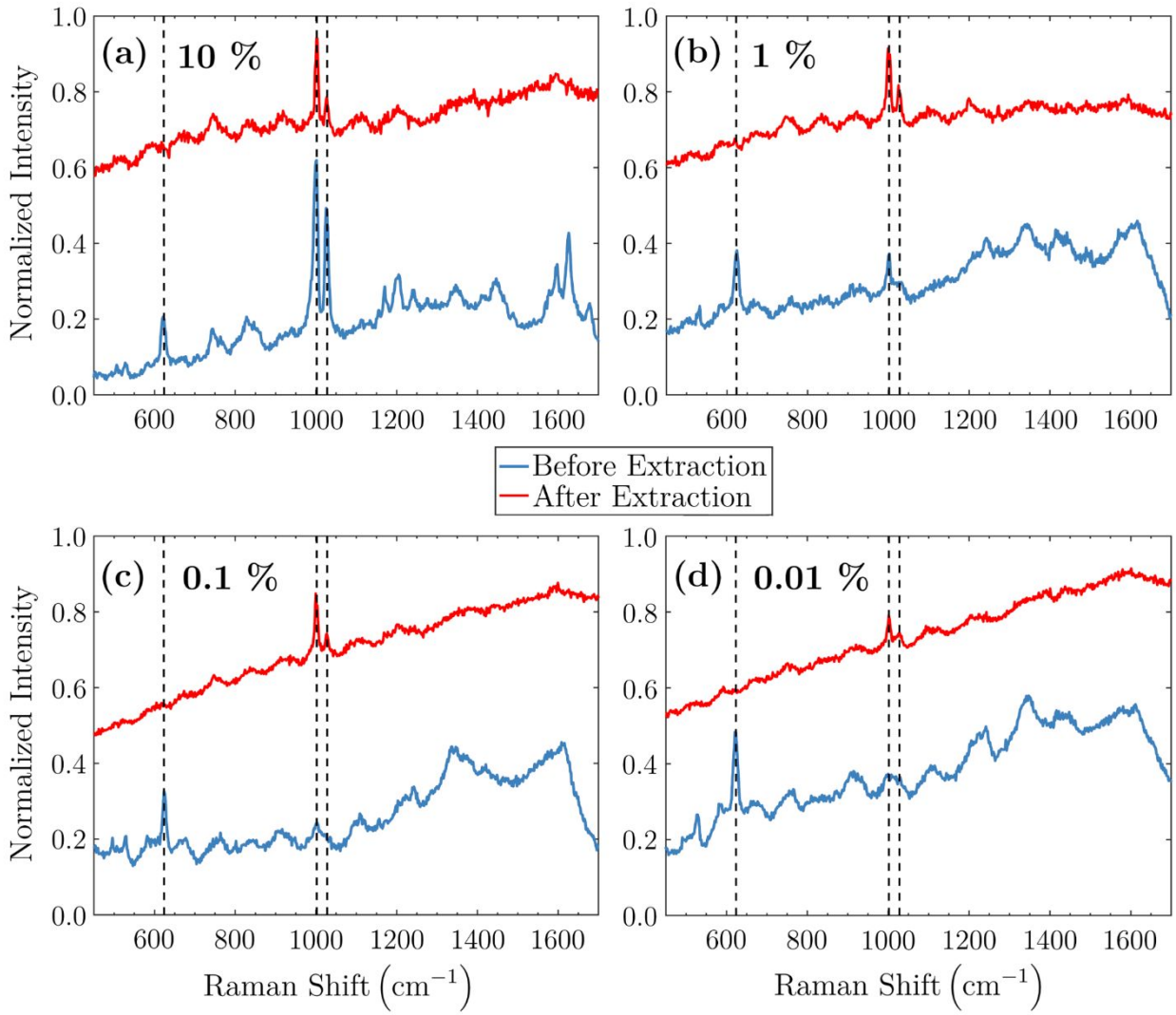

Figure 4. Normalized spectra corresponding to 10% (a), 1% (b), 0.1% (c), 0.01% (d) concentration ratios of fentanyl in heroin hydrochloride in the samples. 'Before Extraction' (control) samples are aqueous whereas 'After Extraction' samples are dispersed in 1:5 mixture of octanol to ethanol. Spectra were normalized by the intensity of Ag-I band at ~118 cm^{-1} (Figure S1), to account for the variability of nanoparticle cluster size between experiments. Peak at 624 cm^{-1} is characteristic of heroin hydrochloride whereas the peaks at 1002 cm^{-1} and 1028 cm^{-1} are assigned to fentanyl. It is clear that extraction significantly improves detection of fentanyl by selectively enriching fentanyl, hence eliminating interference from hydrophilic heroin hydrochloride.

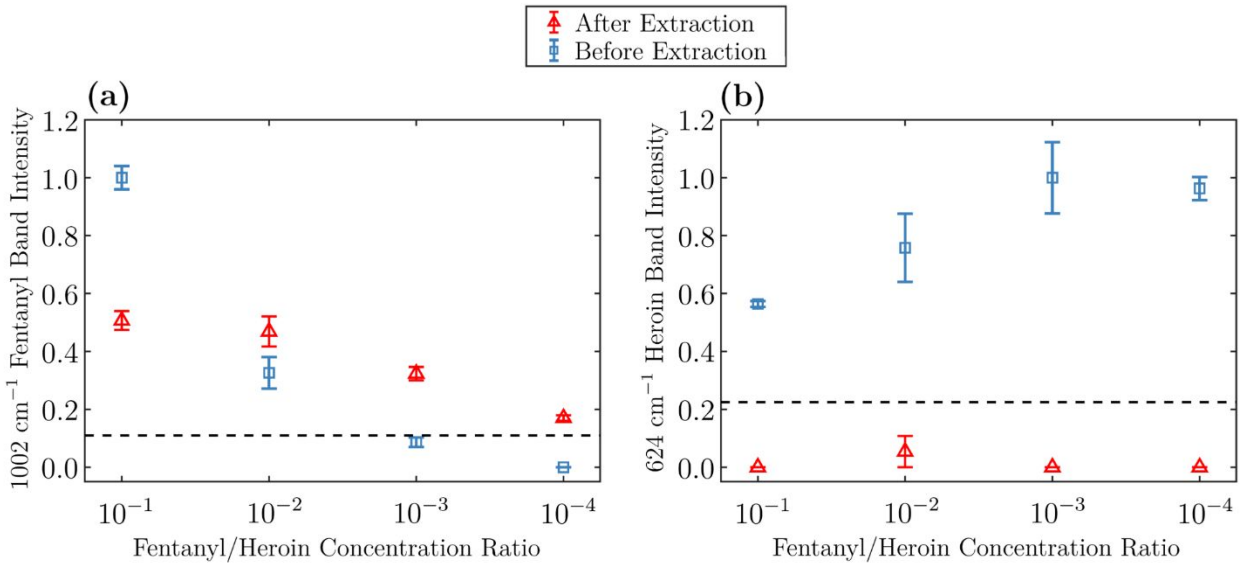

Figure 5. Intensity of the 1002 cm^{-1} band which is assigned to fentanyl (a), and intensity of 624 cm^{-1} band which is assigned to heroin hydrochloride (b). Values are obtained from 4 independent experiments, with error bars corresponding to 95% confidence. Dashed lines correspond to signal-to-noise ratio of 3. Datapoints which fall below the dashed lines are assumed to be unreliable. It is evident that extraction improves detection limit of fentanyl (a) by two orders of magnitude. (b) shows that extraction completely eliminated heroin bands.

Graphical Abstract: